IMPLEMENTATION OF INTERLAMINAR FRACTURE MECHANICS IN DESIGN: AN OVERVIEW

Ronald Krueger
National Institute of Aerospace, Hampton, Virginia

Pierre J. Minguet
The Boeing Company, Philadelphia, Pennsylvania

T. Kevin O'Brien
ARL/VTD, NASA Langley Research Center, Hampton, Virginia

SUMMARY: The state-of-the-art in the areas of delamination characterization, interlaminar fracture mechanics analysis tools and experimental verification of life predictions is demonstrated using skin/stringer debonding failure as an engineering problem to describe the overall methodology.

KEY TERMS: delamination, fracture toughness, computational fracture mechanics, finite element analysis, virtual crack closure technique

INTRODUCTION

Many composite components in aerospace structures are made of flat or curved panels with co-cured or adhesively-bonded frames and stiffeners. A consistent step-wise approach has been developed over the last decade which uses experiments to detect the failure mechanism, computational stress analysis to determine the location of first matrix cracking and computational fracture mechanics to investigate the potential for delamination growth. Testing of thin skin stiffened panels designed for aircraft fuselage applications has shown that bond failure at the tip of the frame flange is an important and very likely failure mode as shown in Figure 1 [1]. Debonding also occurs when a thin-gage composite fuselage panel is allowed to buckle in service. Comparatively simple specimens consisting of a stringer flange bonded onto a skin have been developed to study skin/stiffener debonding [2, 3] (Figure 2a). The failure that initiates at the tip of the flange in these specimens (as shown in Figure 2b) is identical to the failure observed in the full-scale panels and the frame pull-off specimens [1, 4].

The objective of this paper is to demonstrate the state-of-the-art in the areas of delamination characterization, interlaminar fracture mechanics analysis tools and experimental verification of life predictions. The advances required in all three areas in order to reach the level of maturity desired for implementation of this methodology for design and certification of composite components are highlighted. The skin/stringer debonding failure was selected as an engineering problem to demonstrate the overall methodology.

INTERLAMINAR FRACTURE MECHANICS

Interlaminar fracture mechanics has proven useful for characterizing the onset and growth of delaminations [5-7]. The total strain energy release rate, G_T, the mode I component due to interlaminar tension, G_I, the mode II component due to interlaminar sliding shear, G_{II}, and the mode III component,

Presented at 14th International Conference on Composite Materials (ICCM-14), San Diego, July 14-18, 2003.

G_{III}, due to interlaminar scissoring shear, as shown in Figure 3, need to be calculated. In order to predict delamination onset or growth for two-dimensional problems, these calculated G components are compared to interlaminar fracture toughness properties measured over a range of mode mixities from pure mode I loading to pure mode II loading [8-11]. A quasi static mixed-mode fracture criterion is determined by plotting the interlaminar fracture toughness, G_c, versus the mixed-mode ratio, G_{II}/G_T, determined from data generated using pure Mode I DCB (G_{II}/G_T=0), pure Mode II 4ENF (G_{II}/G_T=1), and mixed-mode MMB tests of varying ratios as shown in Figure 4. A curve fit of these data is performed to determine a mathematical relationship between G_c and G_{II}/G_T. Failure is expected when, for a given mixed mode ratio G_{II}/G_T, the calculated total energy release rate, G_T, exceeds the interlaminar fracture toughness, G_c. In order to predict delamination onset or growth for three-dimensional problems the entire failure surface $G_c=G_c$ (G_I, G_{II}, G_{III}) as shown in Figure 5 is required. Although several specimens have been suggested for the measurement of the mode III interlaminar fracture toughness property [12-14], an interaction criterion incorporating the scissoring shear, however, has not yet been established. The edge-cracked torsion test (ECT) appears to be the most likely candidate for standardization [15].

The methodology has been extended to predict fatigue delamination onset life [4, 16, 17] but to date a standard only exists for the Mode I DCB test [18]. Interlaminar fracture mechanics has also been used to characterize the extension or growth of delaminations when subjected to fatigue loading [19]. In analogy with metals, delamination growth rate can therefore be expressed as a power law function. However, the exponent is typically high for composite materials compared to metals and standards for the measurement of fatigue delamination growth have not yet been established [20]. In view of the uncertainties related to the high exponents of the delamination grow rate, it has been suggested to design to levels below a threshold stain energy release rate to ensure no delamination growth.

ANALYSIS TOOLS

A variety of methods are used to compute the strain energy release rate based on results obtained from finite element analysis. For delaminations in laminated composite materials where the failure criterion is highly dependent on the mixed-mode ratio (as shown in Figure 4) the virtual crack closure technique (VCCT) [21, 22] has been most widely used for computing energy release rates. Results base on continuum (2-D) and solid (3-D) finite element analyses provide the mode separation required when using the mixed-mode fracture criterion.

The mode I, and mode II components of the strain energy release rate, G_I, G_{II} are computed as shown in Figure 6 for a 2-D eight-noded element as an example of VCCT. The terms X'_i, Z'_i are the forces at the crack tip at nodal point i and u'_ℓ, w'_ℓ (u'_{ℓ^*}, w'_{ℓ^*}) are the displacements at the corresponding nodal points ℓ and ℓ^* behind the crack tip. Similar definitions are applicable for the forces at nodal point j and displacements at nodal points m and m^*. For geometric nonlinear analysis where large deformations may occur, both forces and displacements obtained in the global coordinate system need to be transformed into a local coordinate system (x', z') which originates at the crack tip as shown in Figure 6. The local crack tip system defines the tangential (x', or mode II) and normal (z', or mode I) coordinate directions at the crack tip in the deformed configuration. The extension to 3-D is straight forward and the total energy release rate G_T is calculated from the individual mode components as $G_T = G_I + G_{II} + G_{III}$, where $G_{III} = 0$ for the two-dimensional case shown in Figure 6.

In spite of its simplicity, the virtual crack closure technique has been used mainly by scientists in universities, research institutions and government laboratories and is usually implemented in their own specialized codes or used in post-processing routines in conjunction with general purpose finite element codes [22]. A more widely spread application of the methodology for the prediction of delamination onset and growth described above is hindered today by the fact that the virtual crack closure technique has not yet been implemented into any of the large commercial general purpose finite element codes such as MSC NASTRAN, ABAQUS, and ANSYS which are used in industry. In order to increase the use and acceptance of the methodology described, it will be necessary to implement VCCT as an integral part of a finite element code including appropriate input capabilities which allow simple definition of a 2-D crack

front or a 3-D delamination contour. The implementation of suitable graphical output for post processing such as arrow plots is also required. For delamination propagation analysis and the determination of the shape of a growing front adaptive mesh refinement techniques and the implementation of a moving mesh algorithm will be required [23].

EXPERIMENTAL VERIFICATION OF LIFE PREDICTION METHOD

The methodology based on fracture mechanics has been used with limited success in the past primarily to investigate delamination onset and debonding in fracture toughness specimens (such as Double Cantilever Beam Specimen) and laboratory size coupon type specimens (such as the skin/stringer debond specimen) as shown in Figure 7. Future acceptance of the methodology by industry and certification authorities however, requires the successful demonstration of the methodology on subcomponent and eventually structural level such as a stringer stiffened panel shown in Figure 7.

On coupon size level, the current focus has been on testing and modeling of the skin/stiffener debond specimen which consisted of a bonded skin and flange assembly as shown in Figure 2a. Quasi-static tension and fatigue tests as well as static three-point bending test (as shown in Figure 7) were performed. The tests were terminated when the flange debonded from the skin. Damage was documented from photographs of the polished specimen edges at each of the four flange corners identified in Figure 2b. The damage at corners 2 and 3, formed first and consisted of a matrix crack in the 45º skin surface ply and a delamination at the +45º/-45º interface [4]. The deformed three-dimensional model of the specimen with load and boundary conditions is shown in Figure 8a. The specimen was modeled using ABAQUS® solid twenty-noded hexahedral elements C3D20R. For the simulation of the tension test, a two-dimensional model was extruded into twenty elements across the width of the specimen, with a refined zone near the free edges as shown in Figures 4b. The fact that the delamination changed across the specimen width from a delamination running at the skin surface 45°/-45° layer interface to a delamination propagating in the bondline above (see Figure 2b), however, was not accounted for in this model. Nevertheless, the three-dimensional model takes width effects into account and, therefore, provided insight into the limitations of the use of the two-dimensional finite element models used earlier [24].

During a series of nonlinear finite element analyses, strain energy release rates were computed at each front location for the loads applied in the experiments. A three-dimensional plot of the distribution of the energy release rate across the width of the specimen is shown in Figure 8c. Along the length (x-coordinate) it was observed that after a small initial drop the computed total energy release rate increases sharply with delamination length, reaches a peak value and gradually decreases. Across the width (z-coordinate) the computed total energy release rate gradually increases with z before it first drops off near the free edges and then sharply increases in the zone of the mesh refinement in the immediate vicinity of the free edges (z=0.0 mm and z=25.4 mm). For three-dimensional analysis, G_S is introduced, which denotes the sum of the in-plane shearing components G_{II}+G_{III}. Also the definition of the mixed-mode ratio is modified to G_S /G_T. For two-dimensional analyses, where G_{III}=0, this definition is equal to the previously used definition of the mixed mode ratio, G_{II}/G_T. A three-dimensional plot of the distribution of the mixed-mode ratio G_S/G_T across the width of the specimen is shown in Figure 8d. Along the length (x-coordinate) it was observed that the delamination initially starts with high shearing components, followed by a drop which is equivalent to an increase in opening mode I. For longer delaminations a gradual increase in shearing components is observed. Across the width (z-coordinate) the computed mixed mode ratio indicated high shearing components near the edges, followed by a drop toward the center of the specimen, which is equivalent to an increase in opening mode I [25].

Three-dimensional finite element models have been used to study the behavior from small scale fracture toughness testing specimens as shown in Figure 9a to larger and more complex coupon size specimens discussed above. Since many layers of brick elements through the specimen thickness are often necessary to model the individual plies, the size of finite element models required for accurate analyses may become prohibitively large as demonstrated in the example of the skin/stringer specimen. For detailed modeling and analysis of the damage observed during the experiments, therefore, a shell/3-D

modeling technique appears to offer a great potential for saving modeling and computational effort because only a relatively small section in the vicinity of the delamination front needs to modeled with solid elements. The technique combines the accuracy of the full three-dimensional solution with the computational efficiency of a plate or shell finite element model, which has been demonstrated for various applications [26]. The deformed shell/3-D model of the skin/stringer specimen subjected to three-point bending is shown in Figure 9b. The global section was modeled with ABAQUS® reduced integrated eight-noded quadrilateral shell elements S8R. The local three-dimensional model extended about three skin thicknesses on the side where the delamination originated from the matrix crack in the top 45º skin surface ply and extended to about three skin plus flange thicknesses beyond the maximum delamination length modeled. The local three-dimensional section was almost identical to the equivalent segment of the full three-dimensional model shown in Figure 8. Computed total strain energy release rates and mixed mode ratios were in good agreement with the results from full 3-D analysis. Details of the analysis are given in reference [25].

For the successful demonstration of the methodology on structural level the stringer stiffened panel shown in Figure 7 was selected. The 1,016-mm by 1,016-mm wide panel is reinforced with three stringers and is subjected to pure shear loading which causes the panel to buckle. The resulting out-of-plane deformation initiates the skin/stringer separation. The deformed shell model of the stringer stiffened panel with load and boundary conditions is shown in Figure 9c. The shell/3-D modeling technique offers great potential for limiting the model size because only a relatively small section in the vicinity of the delamination front needs to be modeled with solid elements. Only the debonded section at the termination of the center stiffener (as shown in the detail) is replaced by a local three-dimensional model. The local three-dimensional model is used to obtain forces and displacements at the delamination front to perform VCCT. The remaining structure stays unaffected which results in a shell/3-D model similar to the model of the skin/stringer specimen shown in Figure 9b. Computed total strain energy release rates and mixed mode ratios are computed for a range of delamination lengths and correlated to the mixed-mode failure criterion in Figure 4. This task is currently performed under the Survivable, Affordable, Reparable Airframe Program (SARAP).

CONCLUDING REMARKS

Progress has been made in the areas of delamination characterization, interlaminar fracture mechanics analysis tools and experimental verification of life predictions. A methodology based on interlaminar fracture mechanics has been applied with limited success to investigate delamination onset and debonding in fracture toughness specimens and laboratory size coupon type specimens based on rotorcraft dynamic and airframe components. Future acceptance of the above methodology by industry and certification authorities requires advances in all areas in order to reach the level of maturity desired for implementation of this methodology for design and certification of composite components.

REFERENCES

[1] P. J. Minguet, M. J. Fedro, T. K. O'Brien, R. H. Martin, and L. B. Ilcewicz, "Development of a Structural Test Simulating Pressure Pillowing Effects in Bonded Skin/Stringer/Frame Configuration," in *Fourth NASA/DoD Advanced Composite Technology Conference*, 1993.

[2] P. J. Minguet and T. K. O'Brien, "Analysis of Composite Skin/Stringer Bond Failures Using a Strain Energy Release Rate Approach," in *The Tenth International Conference on Composite Materials*, vol. I, A. Poursartip and K. Street, Eds., 1995, pp. 245-252.

[3] P. J. Minguet and T. K. O'Brien, "Analysis of Test Methods for Characterizing Skin/Stringer Debonding Failures in Reinforced Composite Panels," in *Composite Materials: Testing and Design (Twelfth Volume), ASTM STP 1274*, 1996, pp. 105-124.

[4] R. Krueger, I. L. Paris, T. K. O'Brien, and P. J. Minguet, "Fatigue Life Methodology for Bonded Composite Skin/Stringer Configurations," *J. of Comp. Tech. and Res.*, vol. 24, pp. 56-79, 2002.

[5] T. K. O'Brien, "Characterization of Delamination Onset and Growth in a Composite Laminate," in *Damage in Composite Materials, ASTM STP 775*, 1982, pp. 140-167.

[6] T. K. O'Brien, "Interlaminar fracture toughness: The long and winding road to standardization," *Composites Part B*, vol. 29, pp. 57-62, 1998.
[7] R. H. Martin, "Incorporating interlaminar fracture mechanics into design," in *International Conference on Designing Cost-Effective Composites*: IMechE Conference Transactions, London, U.K., 1998, pp. 83-92.
[8] "ASTM D 5528-94a, Standard Test Method for Mode I Interlaminar Fracture Toughness of Unidirectional Fiber-Reinforced Polymer Matrix Composites," in *Annual Book of ASTM Standards*, vol. 15.03: American Society for Testing and Materials, 2000.
[9] R. H. Martin and B. D. Davidson, "Mode II Fracture Toughness Evaluation Using A Four Point Bend End Notched Flexure Test," *Plastics, Rubber and Composites*, vol. 28, pp. 401-406, 1999.
[10] J. R. Reeder and J. H. Crews, "Mixed Mode Bending Method for Delamination Testing," *AIAA J.*, vol. 28, pp. 1270--1276, 1990.
[11] J. R. Reeder and J. H. Crews, "Redesign of the Mixed-Mode Bending Delamination Test to Reduce Nonlinear Effects," *Journal Composite Tech. Res.*, vol. 14, pp. 12--19, 1992.
[12] S. M. Lee, "An Edge Crack Torsion Method for Mode III Delamination Fracture Testing," *J. of Composite Technology and Research.*, pp. 193--201, 1993.
[13] R. H. Martin, "Evaluation of the Split Cantilever Beam for Mode III Delamination Testing," in *Composite Materials: Fatigue and Fracture (Third Volume), ASTM STP 1110*, 1991, pp. 243-266.
[14] P. Robinson and D. Q. Song, "Development of an improved mode III delamination test for composites," *Composites Science and Technology*, vol. 52, pp. 217-233, 1994.
[15] J. Li, S. M. Lee, E. W. Lee, and T. K. O'Brien, "Evaluation of the Edge Crack Torsion ECT Test for Mode III Interlaminar Fracture Toughness of Laminated Composites," *Journal of Composites Technology and Research*, vol. 19, pp. 174-183, 1997.
[16] T. K. O'Brien, "Towards a Damage Tolerance Philosophy for Composite Materials and Structures," in *Composite Materials Testing and Design (Ninth Volume), ASTM STP1059*, S. P. Garbo, Ed., 1990, pp. 7-33.
[17] G. B. Murri, T. K. O'Brien, and C. Q. Rousseau, "Fatigue Life Methodology for Tapered Composite Flexbeam Laminates," *Journal of the American Helicopter Society*, vol. 43, pp. 146--155, 1998.
[18] "ASTM D 6115-97, Standard Test Method for Mode I Fatigue Delamination Growth Onset of Unidirectional Fiber-Reinforced Polymer Matrix Composites," in *Annual Book of ASTM Standards*, vol. 15.03: American Society for Testing and Materials, 2000.
[19] D. M. Hoyt, S. H. Ward, and P. J. Minguet, "Strength and Fatigue Life Modeling of Bonded Joints in Composite Structure," *J. of Comp. Tech. and Res.*, vol. 24, pp. 190-210, 2002.
[20] R. H. Martin and G. B. Murri, "Characterization of Mode I and Mode II Delamination Growth and Thresholds in AS4/PEEK Composites," in *Composite Materials: Testing and Design (Ninth Volume), ASTM STP 1059*, 1990, pp. 251--270.
[21] E. F. Rybicki and M. F. Kanninen, "A Finite Element Calculation of Stress Intensity Factors by a Modified Crack Closure Integral," *Eng. Fracture Mech.*, vol. 9, pp. 931-938, 1977.
[22] R. Krueger, "The Virtual Crack Closure Technique: History, Approach and Applications,", NASA/CR-2002-211628, ICASE Report No. 2002-10, May 2002.
[23] S. Rinderknecht and B. Kröplin, "Delamination Growth Simulation with a Moving Mesh Technique," in *Advances in Non-Linear Finite Element Methods*, B. H. V. Topping and M. Papadrakakis, Eds., 1994, pp. 187-197.
[24] R. Krueger, I. L. Paris, T. K. O'Brien, and P. J. Minguet, "Comparison of 2D Finite Element Modeling Assumptions with Results from 3D Analysis for Composite Skin-Stiffener Debonding," *Composite Structures*, vol. 57, pp. 161-168, 2002.
[25] R. Krueger and P. J. Minguet, "Analysis of Composite Skin-stiffener Debond Specimens Using Volume Elements and a Shell/3D Modeling Technique," NASA/CR-2002-211947, 2002.
[26] R. Krueger and T. K. O'Brien, "A Shell/3D Modeling Technique for the Analysis of Delaminated Composite Laminates," *Composites Part A*, vol. 32, pp. 25-44, 2001.

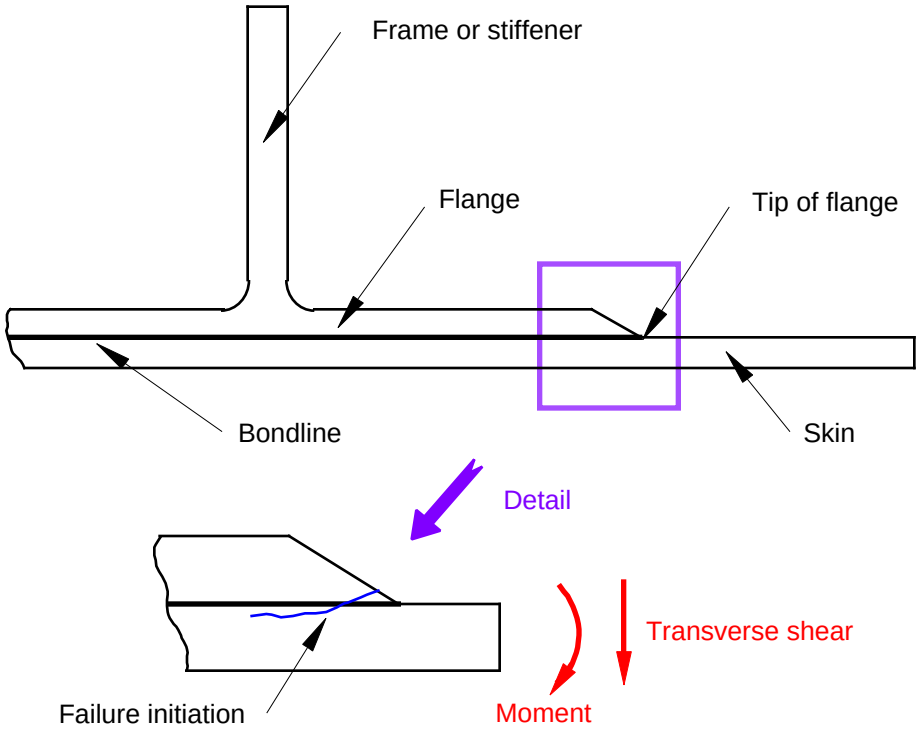

Figure 1: Cobonded skin/stringer configuration with typical failure at flange tip.

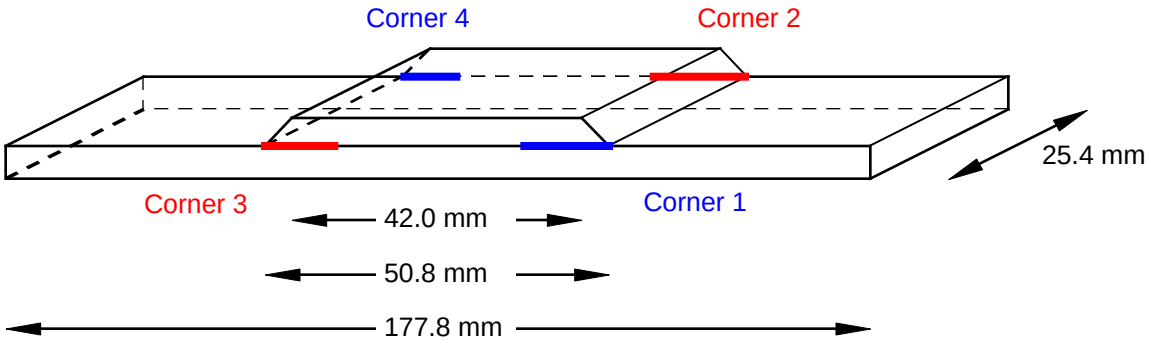

(a) Specimen configuration.

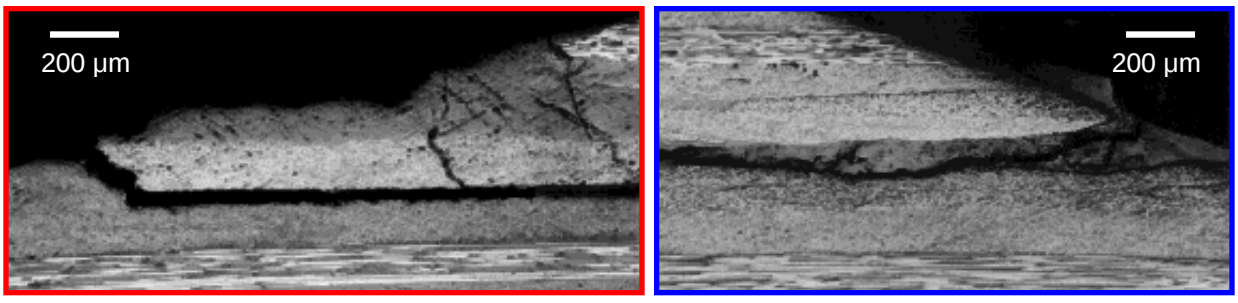

Damage patterns at corners 2 and 3 Damage patterns at corner 1 and 4

(b) Micrograph of the edges of a failed specimen.

Figure 2: Skin/stringer debond specimen.

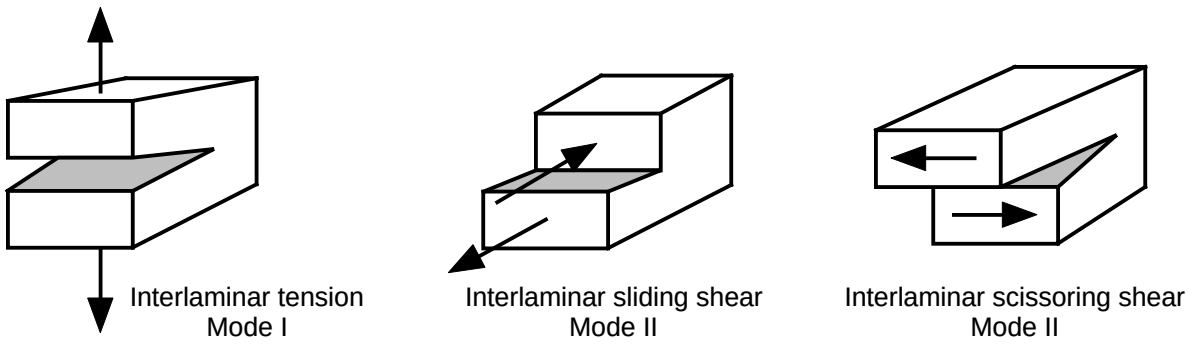

Figure 3: Fracture Modes.

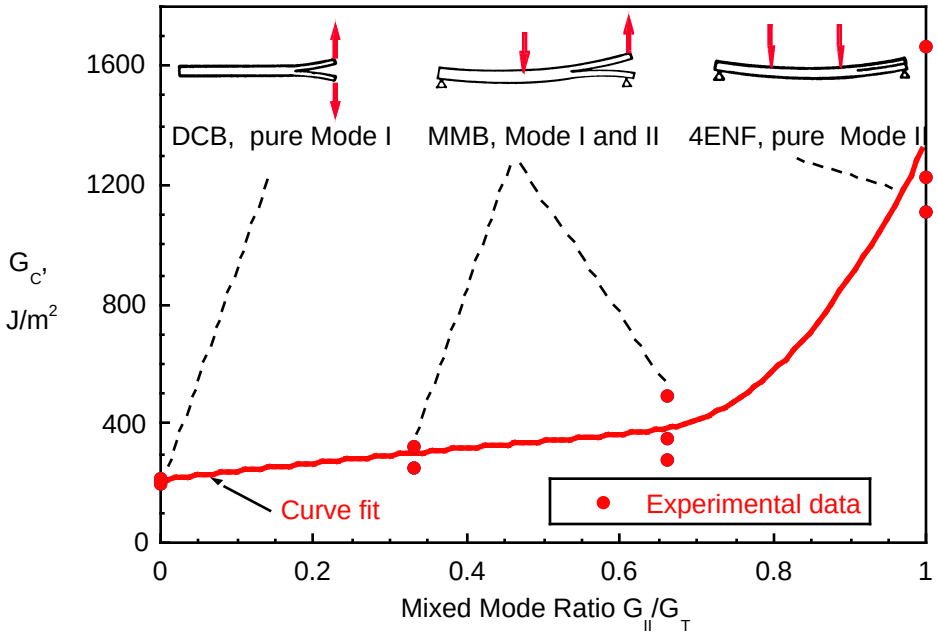

Figure 4: Mixed mode I, II failure criterion for IM7/8552.

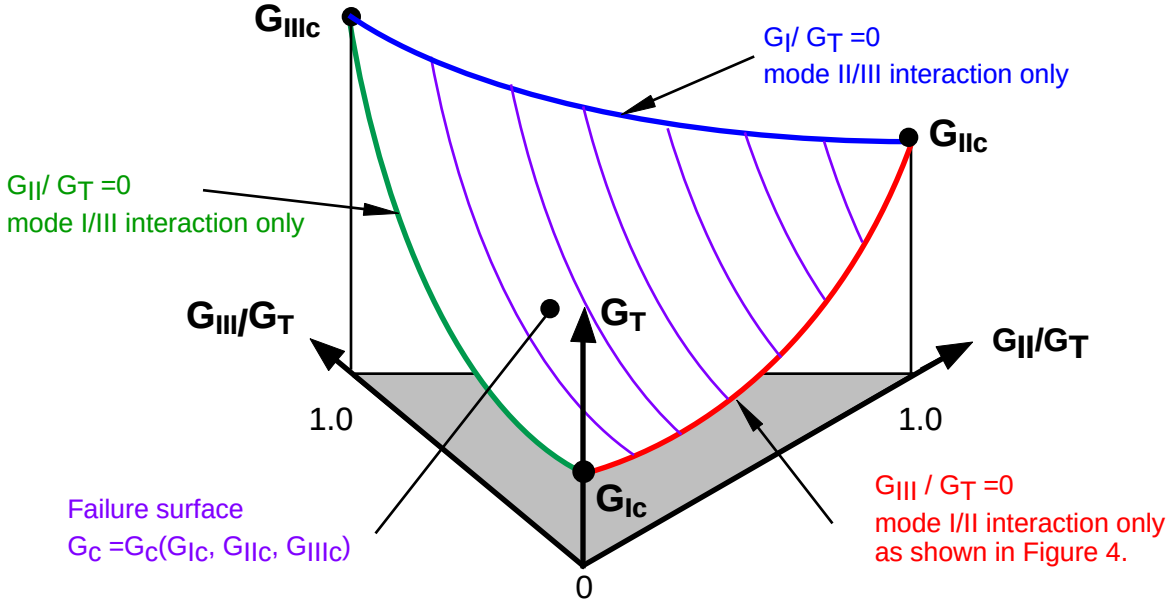

Figure 5: Mixed mode failure criterion for modes I, II and III.

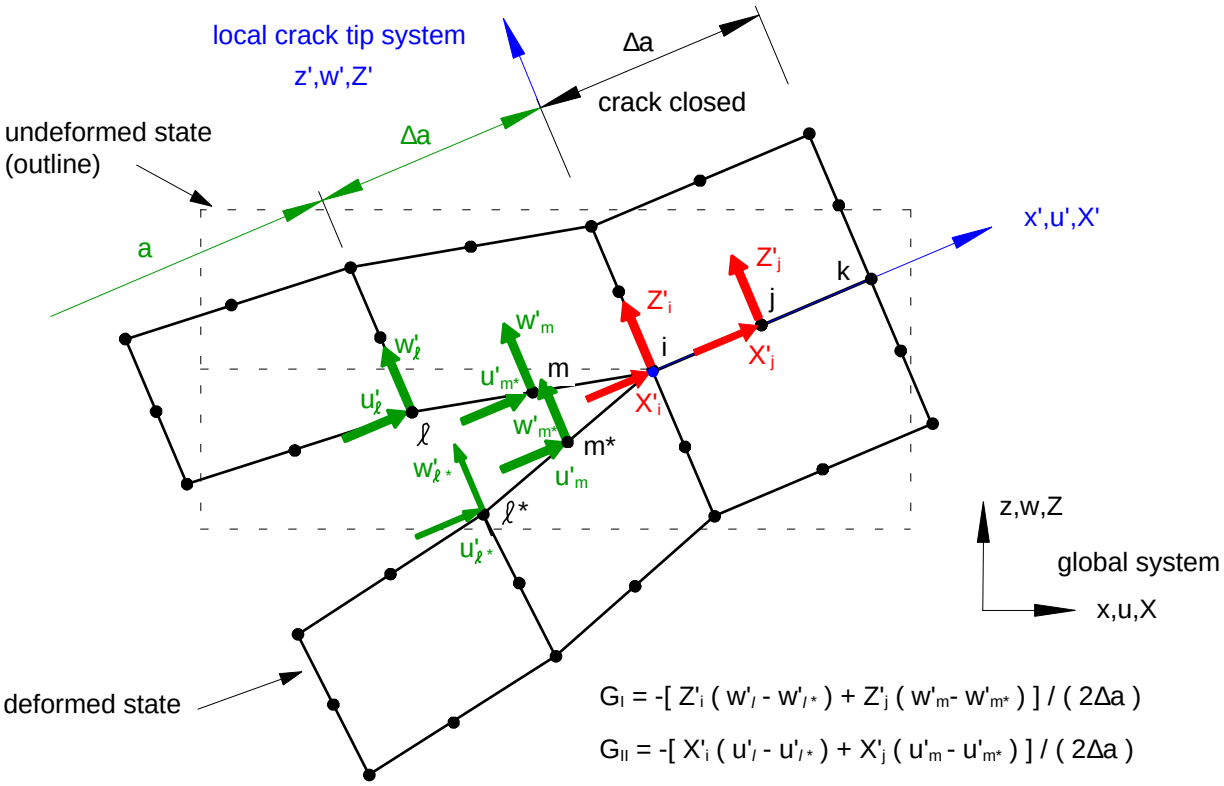

Figure 6: Virtual Crack Closure Technique (VCCT) for geometrically nonlinear analysis.

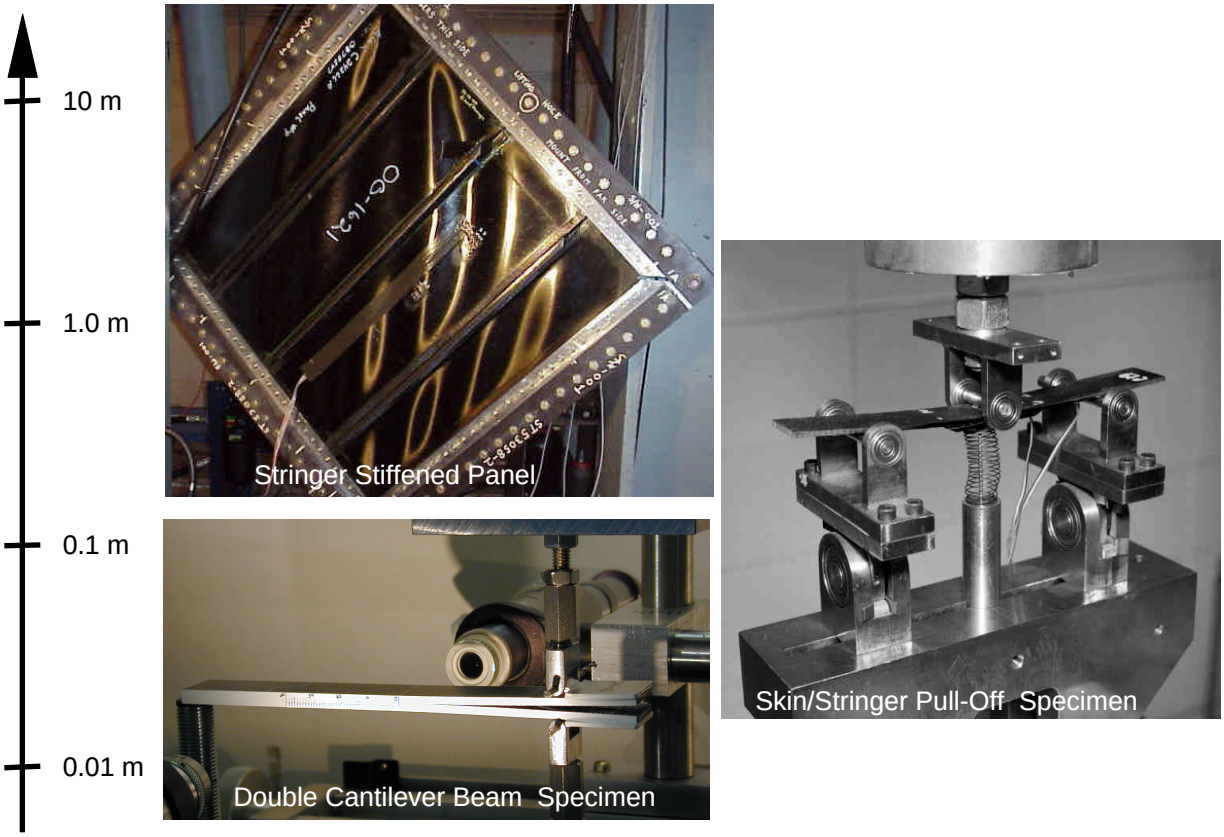

Figure 7: Testing from characterization specimen to structural component.

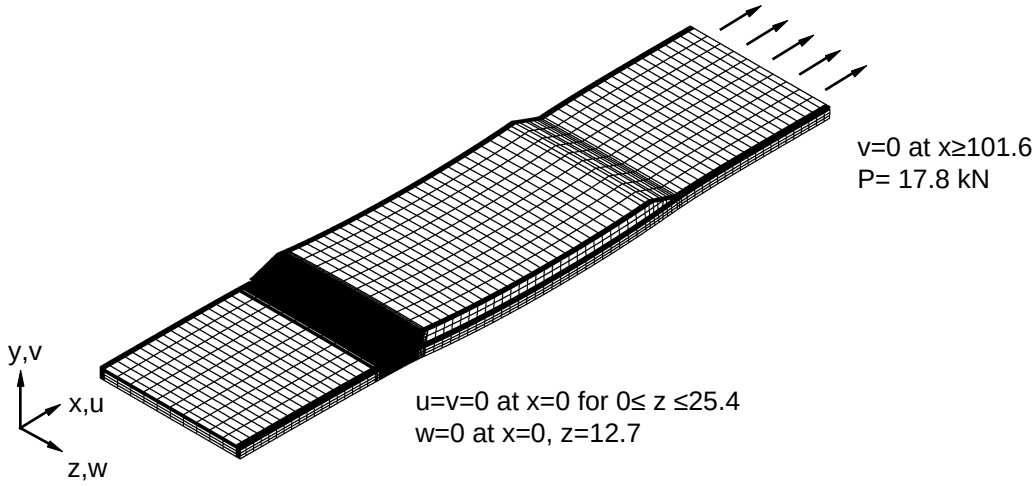

(a) Deformed three-dimensional model of skin/stringer specimen with load and boundary conditions.

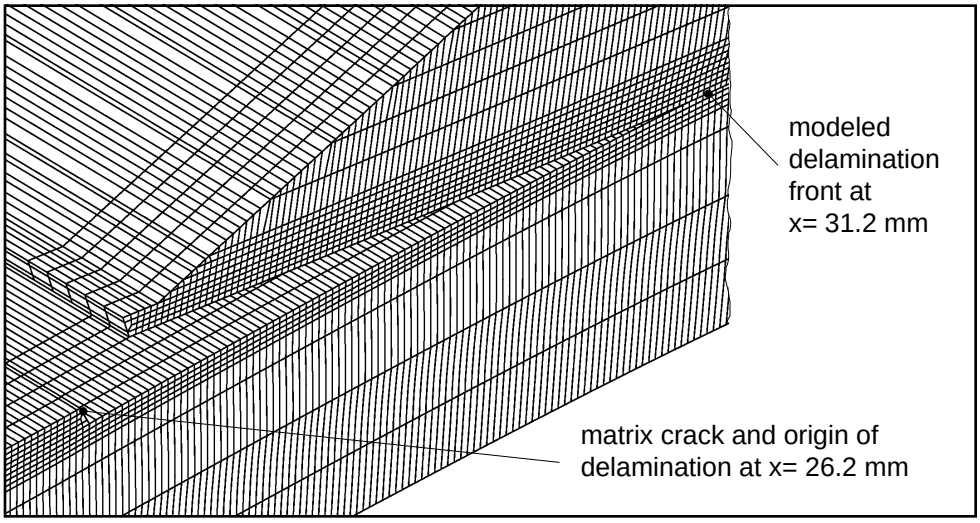

(b) Detail of deformed model of damaged specimen in the vicinity of the flange tip.

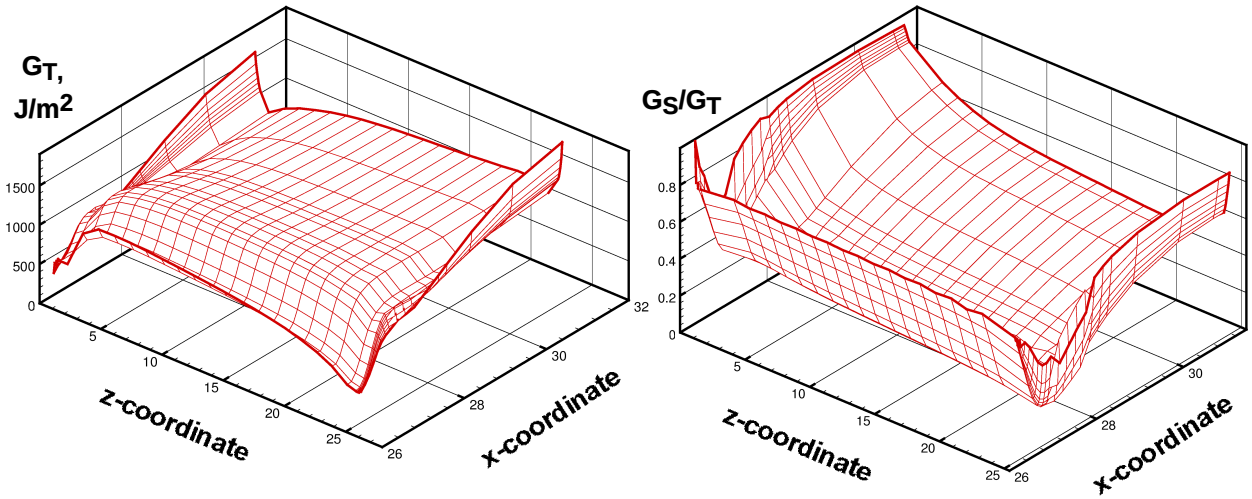

(c) Computed total energy release rate distribution. (d) Computed mixed mode ratio G_S/G_T distribution.

Figure 8. Full three-dimensional FE analysis of skin/stringer specimen subjected to tension loading.

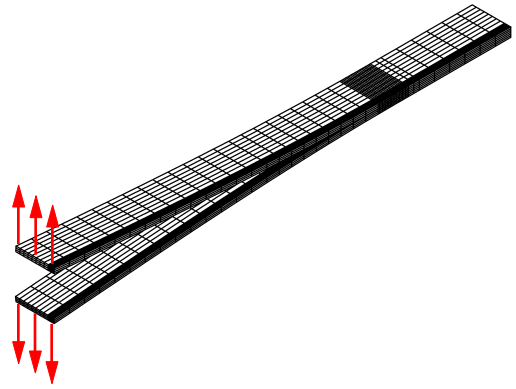

(a) Full 3D model of a DCB specimen

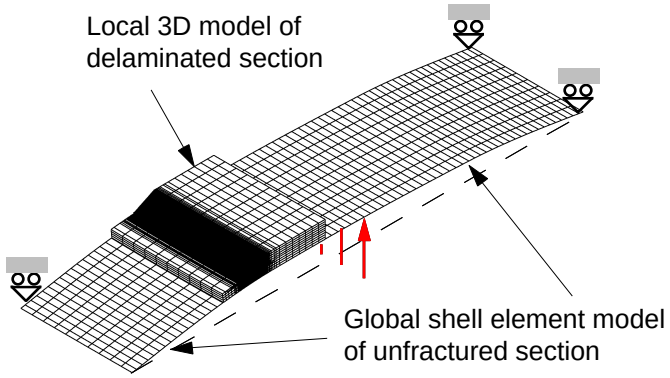

(b) Shell/3D model of a skin/stringer specimen

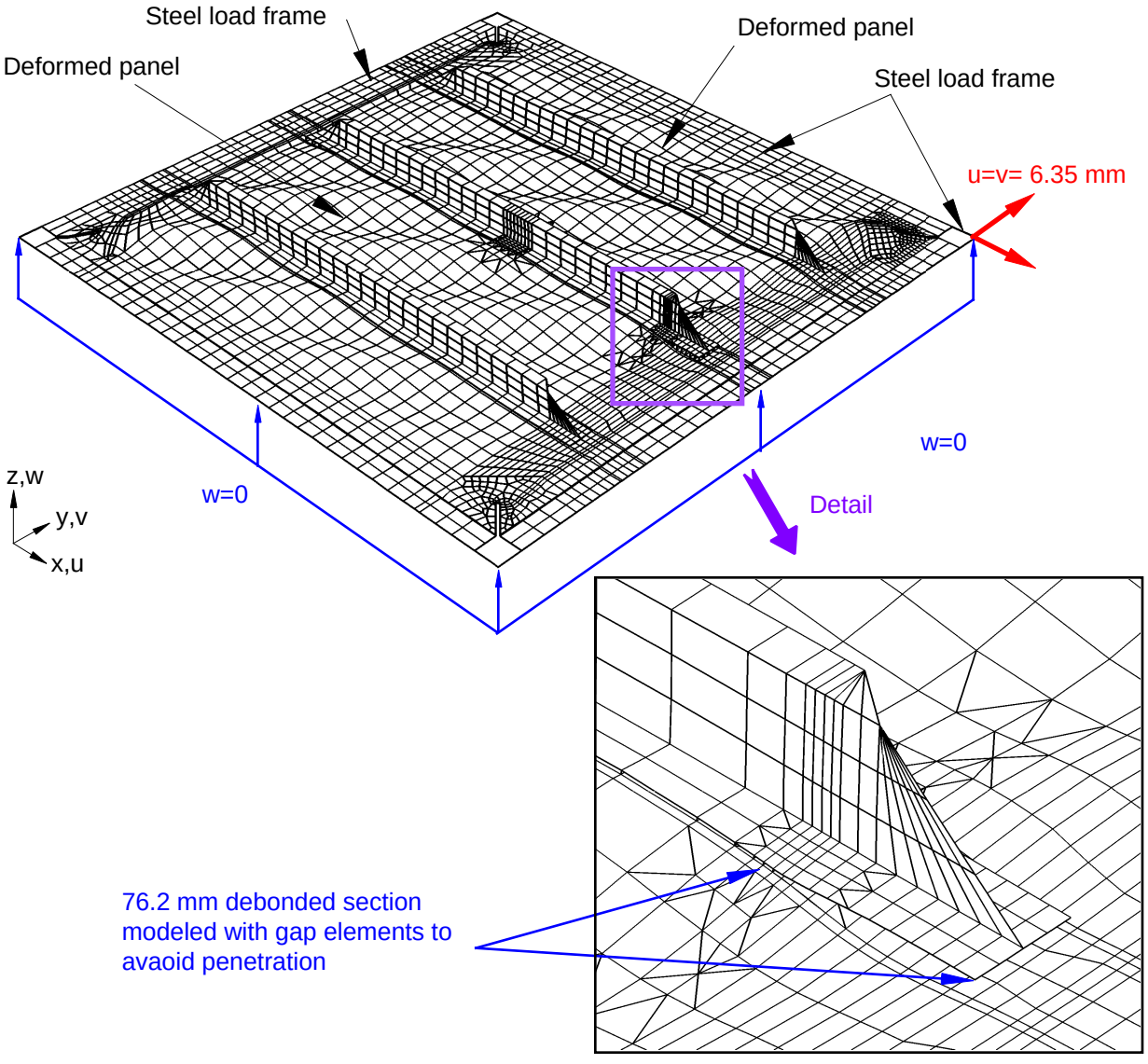

(c) Shell model of stringer stiffened panel under shear loading with detail of debonded center stringer

Figure 9: Finite element analyses of different complexity.